



ELSEVIER

27 September 1999

PHYSICS LETTERS A

Physics Letters A 260 (1999) 495–501

www.elsevier.nl/locate/physleta

Induction accelerator for crystalline beams

R. Blümel^{*}, P.E. Smaldino

Department of Physics, Wesleyan University, Middletown, CT 06459-0155, USA

Received 5 July 1999; received in revised form 12 August 1999; accepted 18 August 1999

Communicated by B. Fricke

Abstract

A quadrupole ring trap and a betatron are combined to form a new type of induction accelerator (crystron) that allows stable acceleration of crystalline ion chains. We illustrate the working principle and the stability of the crystron by simulating numerically the acceleration of chains of up to 1000 crystallized $^{24}\text{Mg}^+$ ions. © 1999 Elsevier Science B.V. All rights reserved.

Experimenting with a set of floating magnets Mayer demonstrated more than a century ago that the stable equilibrium configurations of trapped charged particles exhibit regular geometric patterns [1,2]. In the context of early atomic models, Mayer's ideas were developed further by Thomson [3] and Föppl [4] and eventually led to the experimental demonstration of macroscopic [5] and microscopic [6,7] Coulomb crystals in electrodynamic traps. A qualitatively new idea was introduced in 1985 by Schiffer and Kienle [8] who proposed to create fast beams of crystallized heavy ions. An important milestone on the way to crystalline beams was the demonstration of macroscopic stationary crystalline structures of laser-cooled $^{24}\text{Mg}^+$ ions in an rf ring trap [9–11] by a research group at the Max-Planck-Institute for Quantum Optics in Munich (MPQ). In 1996 strong experimental indications for the existence of fast Coulomb-ordered chains were found by

Steck and collaborators [12–14] who experimented with electron-cooled beams [15,16] of heavy ions at the ESR storage ring at GSI in Darmstadt. That the ions in the ESR experiments are indeed ordered has recently been verified theoretically by Hasse [17]. An interesting research direction is currently being pursued by another research group in Munich [18]. This group is currently constructing an improved version (PALLAS) [18] of the successful MPQ ring trap [9–11]. The PALLAS collaboration plans to achieve particle acceleration with the help of drift tubes. The feasibility of this acceleration scheme was recently proved with the help of molecular dynamics computations [18] simulating the acceleration of a hot beam of 200 $^{24}\text{Mg}^+$ ions to speeds of ≈ 5000 m/s. Fast crystalline beams are interesting for many reasons [15]. They offer, for example, the prospect of creating beams of unprecedented quality and brilliance [8–15,17,18]. They may also be used for testing experimentally the suppression of synchrotron radiation of fast crystalline beams [19–21]. We note that all beam crystallization schemes employed so far [8–15,17,18] start with a fast, hot, disordered beam

^{*} Corresponding author. Tel.: +1-860-685-2032; fax: +1-860-685-2031; e-mail: rblumel@wesleyan.edu

which is then acted upon by a cooling mechanism (e.g. laser cooling [15,22,23] or electron cooling [15,16]) in order to form a crystalline beam.

In this Letter we study the production and acceleration of crystalline beams of fast heavy ions of mass m and charge Ze by starting with a crystal at rest and subsequently accelerating the crystal in such a way that the crystalline order is preserved. This acceleration scheme was first suggested in Ref. [20]. In order to achieve this goal we propose a new type of accelerator: a combination of a circular quadrupole rf ring trap and a betatron, the crystron. On the basis of detailed molecular dynamics calculations we demonstrate below that the crystron is indeed capable of accelerating heavy ion crystals to high speeds while preserving the crystalline structure. Thus the proposed accelerator is a good candidate for producing fast crystalline beams in the laboratory. Preliminary computations indicate that the crystron is also capable of producing and accelerating three-dimensional crystalline beams.

A schematic sketch of the crystron is shown in Fig. 1. The basic structure of the machine consists of a cylindrical induction transformer B (betatron) [24–27]. A circular evacuated tube located in the gap G between the poles P and Q of the transformer contains a circular rf ring trap T [9–11,18]. A fast ion crystal is generated in this machine according to the following five steps.

1. *Initialization:* The electric current I passed through the induction coil C of the transformer is switched off. The magnetic field in G is zero. The

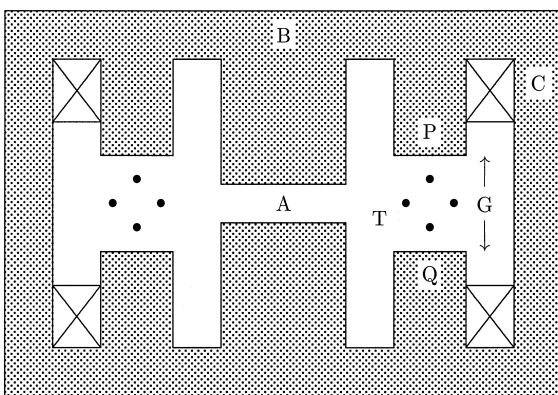


Fig. 1. Schematic sketch of the crystron.

quadrupole ring trap is switched on, i.e. an ac voltage $V_0 \sin(\Omega t)$ and a dc voltage U_0 are applied to the electrodes of the trap. Fig. 1 shows these electrodes schematically as four conducting rods.

2. *Loading:* With the magnetic field switched off and the ring trap switched on (see step 1) the trap is filled with N ions, for instance generated by electron impact ionization of atoms close to the center of the trap's axis [9–11,18]. The ions thus produced form a hot nonneutral plasma.

3. *Crystallization:* Following step 2, a cooling method is now applied to generate an ion crystal in the ring trap. Various cooling schemes are available, e.g. resistive cooling [28], buffer-gas cooling [18], and laser cooling [9–11,15,22,23]. If applicable, laser cooling is by far the most efficient method. In case the considered ion species cannot be cooled directly with lasers, sympathetic cooling [29] may be considered. Steps 2 and 3 have already been proven to work experimentally [9–11], not only for ion chains but also for more complicated three-dimensional crystal configurations.

4. *Preparation:* Once the crystal is obtained, the cooling laser is switched off. In an ultra-high vacuum, where collisions of rest-gas atoms with the crystal can be neglected, this step poses no danger to the ion crystal provided the trap parameters a and q are chosen away from the deterministic melting regions [30,31]. In this case it has been proven experimentally [32,33] and theoretically [34,35] that once the ion crystal is formed, it is safe to switch off the cooling laser without destroying the ion crystal. As a matter of fact, absence of heating following the shut-down of the cooling devices defines a convenient experimental procedure to ascertain the existence of an ion crystal in the trap in case expensive diagnostic equipment (e.g. CCD cameras) is not available [35].

5. *Acceleration:* The ion crystal is now accelerated to its final energy E_f by passing a rising current $I(t)$ through the coil C. The increasing current $I(t)$ generates a time varying magnetic flux $\Phi(t)$ through the circular area enclosed by the ion crystal. This in turn generates an azimuthally directed electric field that accelerates the ion crystal. The crystal is held in its circular orbit by the Lorentz force due to the magnetic field $B(t)$ produced by the poles P and Q in the gap G. In a traditional betatron axial stability

is achieved by means of an inhomogeneous ‘bulging’ magnetic field in the gap G resulting in the weak focusing mechanism of a betatron [24–27]. In a crystron axial stability is provided by the strong focusing effect generated by the circular quadrupole ring trap. Thus in its simplest form a crystron can be built with a *homogeneous* field in the gap G. This is indicated in Fig. 1, where the surfaces of the poles P and Q are shown horizontal and parallel to each other thus generating a homogeneous magnetic field $B(t)$ at the location of the ring trap. This does not mean that crystrons may not benefit from a small amount of weak focusing on top of the strong focusing provided by the ring trap. In a few preliminary numerical simulations we found, however, that stable operation of the crystron is obtained only with a very small magnetic field exponent n [24–27]. This is consistent with the results of other researchers [15] indicating that traditional betatrons are not suitable for creating stable crystalline beams. Great care has to be exercised to fulfill the betatron condition [24–27]. It states that the magnitude of the effective magnetic field enclosed by the circulating crystal must be twice that of the field $B(t)$ generated by P and Q. In an actual machine this condition may be fulfilled by adjusting the width of the air gap A in the central post of the induction magnet [26].

Feasibility and stability of step 5 are now demonstrated with the help of detailed molecular dynamics simulations. The total force acting on an ion during the acceleration step 5 is the sum of the following four forces: the trap force $\mathbf{F}^{(T)}$, the Coulomb force $\mathbf{F}^{(C)}$, the Lorentz force $\mathbf{F}^{(L)}$ and the azimuthal accelerating force $\mathbf{F}^{(A)}$. Choosing $t_0 = 2/\Omega$ as the unit of time, $l_0 = 1 \mu\text{m}$ as the unit of length and introducing the dimensionless time $\tau = t/t_0$, the classical dynamics of N ions in the crystron is described by the following N coupled equations of motion:

$$\frac{d^2 \mathbf{r}_i(t)}{d\tau^2} = \mathbf{F}^{(T)}(\mathbf{r}_i, \tau) + \mathbf{F}^{(C)}(\mathbf{r}_i) + \mathbf{F}^{(L)}(\mathbf{r}_i, \tau) + \mathbf{F}^{(A)}(\mathbf{r}_i, \tau), \quad i = 1, 2, \dots, N, \quad (1)$$

where the position vector $\mathbf{r} = (x, y, z)$ (in units of l_0) refers to a coordinate system whose x - y plane contains the axis of the ring trap and whose z direction

coincides with the axial direction of the crystron. The trap force is explicitly given by

$$\mathbf{F}^{(T)}(\mathbf{r}, \tau) = [a + 2q \cos(2\tau)] \begin{pmatrix} (\rho - R)x/\rho \\ (\rho - R)y/\rho \\ -z \end{pmatrix}, \quad (2)$$

where a and q are the trap control parameters [15] proportional to the dc and ac trap voltages, respectively, $\rho^2 = (x^2 + y^2)$ and R is the radius of the ring trap's axis. The Coulomb force acting on particle number i is given by

$$\mathbf{F}^{(C)}(\mathbf{r}_i) = \kappa \sum_{j \neq i} \frac{\mathbf{r}_i - \mathbf{r}_j}{|\mathbf{r}_i - \mathbf{r}_j|^3}, \quad (3)$$

where $\kappa = Z^2 e^2 / (\pi \epsilon_0 l_0^3 m \Omega^2)$. Assuming a time dependence of

$$B(\tau) = B_0 g(\tau) \quad (4)$$

for the magnetic field in G, the Lorentz force is given by

$$\mathbf{F}^{(L)}(\mathbf{r}, \tau) = \beta g(\tau) \begin{pmatrix} \dot{y} \\ -\dot{x} \\ 0 \end{pmatrix}, \quad (5)$$

where $\beta = 2ZeB_0 / (\Omega m)$. The accelerating force is given by

$$\mathbf{F}^{(A)}(\mathbf{r}, \tau) = \beta \dot{g}(\tau) \begin{pmatrix} y \\ -x \\ 0 \end{pmatrix}. \quad (6)$$

We solved the equations of motion (1) for various particle numbers ranging from $N = 2$ to $N = 1000$ using a numerical fourth order Runge Kutta integrator with constant step size. Since we are interested in accelerating Coulomb crystals, this rather simple integrator turned out to be convenient and efficient for the problem at hand since close Coulomb collisions were not expected to occur. There is no problem to adjust the step size manually in order to obtain converged results.

In all our numerical examples to be discussed below we chose $^{24}\text{Mg}^+$ as the ion species and operated the ring trap at $f = \Omega / (2\pi) = 10$ MHz. We set $a = 0$, $q = 0.2$. The magnetic field was

chosen according to (4) with $B_0 = 1$ T, $g(\tau) = \sin(\omega\tau)$ and $\omega = 0.002$. Thus the acceleration phase 5 of the crystron corresponds to the time interval $0 \leq \tau \leq \tau_{\max} = \pi/(2\omega)$. The radius of the ring trap was chosen to be $R = Nd/(2\pi)$ with $d = 30 \mu\text{m}$. With this choice of trap parameters the crystalline minimal energy configuration is a chain of N ions located on the axis of the ring trap with an ion spacing $s \approx 30 \mu\text{m}$. This corresponds to typical values of ion spacings observed in the MPQ ring trap [9–11].

Initial conditions for the simulation of the acceleration of a crystalline N -ion chain were obtained by placing the ions inside a torus of minor radius $2 \mu\text{m}$ coaxial with the ring trap. While the radial positions of the ions with respect to the trap's axis were chosen randomly, the azimuthal positions of the ions were chosen from a narrow periodic distribution with a mean spacing of $30 \mu\text{m}$. The initial velocities were set to zero.

The numerical solution of the equations of motion (1) provided us with detailed information on the temporal behavior of the phase-space trajectories of the ions in the crystron. We studied ion crystals of sizes $N = 2, 10, 20, 30, 40, 50, 100, 200, 500, 1000$. For all ten cases studied we computed the plasma parameter Γ [36] and found it to be much larger than 200. The plasma parameter stayed above the value 200 during the entire acceleration phase qualifying our ion chains technically as crystals [36]. We also computed the dimensionless linear particle density λ [36] and found it to be approximately 0.25 for all ten crystals studied. This provides a simple consistency test, since Hasse and Schiffer found [36] that the stable crystalline structures for $\lambda < 0.709$ are strings of ions.

Detailed knowledge of the positions of the ions as a function of time allowed us to program an animation of the N -ion crystals displayed on a high-resolution computer terminal. Watching the animations we obtained a qualitative impression of the stability properties of the crystalline ion chains during the acceleration phase. None of the crystals 'exploded'. The crystalline order was clearly preserved over the entire duration of the acceleration phase. Qualitatively there was no difference in the behavior of the ten ion crystals. For all ten crystals studied, the temperatures were much less than 1 mK and the

corresponding ion chains were completely 'frozen'. If the crystron would show any instability at all, one suspects that it would be most pronounced for higher temperatures. Thus we reexamined the $N = 1000$ ion crystal, but this time at much higher temperature corresponding to $\Gamma \approx 3$. The resulting ion chain is technically no longer a crystal, but still well ordered as we will see below. Stability of this 'hot chain' proves that the crystron can be applied successfully even if the thermal fluctuations are large.

The initial distribution of ion spacings of the 'hot' 1000-ion chain is shown in Fig. 2 (a). Although the initial ion velocities were chosen to be zero (see above), the Coulomb interaction between the ions quickly thermalizes the ions to a temperature of about 200 mK. Due to the quasi linear shape of the chain and its closeness to the trap's axis, the trap's rf voltage (rf heating) has practically no effect on its

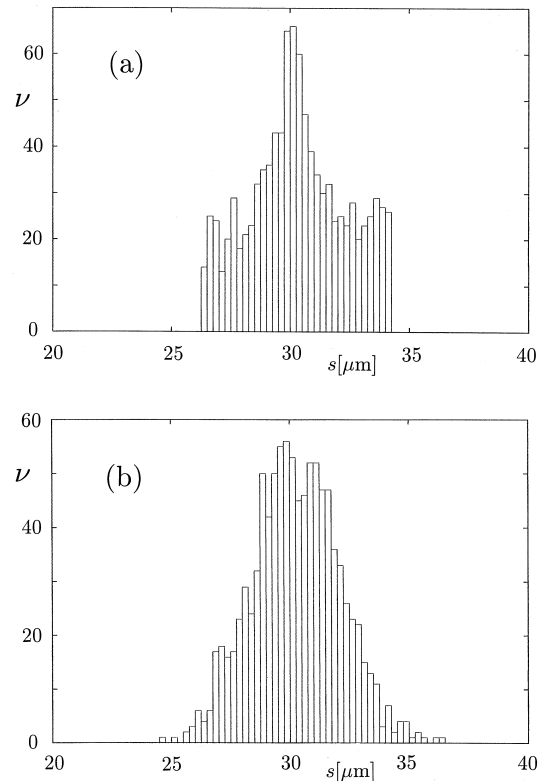


Fig. 2. Probability distribution of ion spacings for the 1000-ion chain. (a) Initial distribution, (b) final distribution of ion spacings after a 25 μs acceleration period in the crystron. ν counts the number of ions in the histogram bins of width 0.25 μm .

temperature. Fig. 3 shows the radial and the axial temperatures of the ion chain as a function of time. The temperatures were computed according to

$$T_\alpha(t) = \frac{m}{2k_B} \langle (\mathbf{v}_\alpha - \mathbf{V}_\alpha)^2 \rangle, \quad (7)$$

where k_B is Boltzmann's constant, $\alpha \in \{\rho, z\}$, $\mathbf{v} = \dot{\mathbf{r}}$, \mathbf{V}_α is the average velocity of the crystal in the α direction and the angular brackets denote an ensemble average over all ions in the crystal. Fig. 3 shows that the temperatures stay roughly constant as a function of time. Due to our choice of initial conditions the temperatures T_ρ and T_z turned out to be different. As shown in Fig. 3, this difference is preserved over the entire acceleration phase. This observation is significant. It shows that there is very little energy exchange between the ρ and the z directions. As a result these two degrees of freedom are essentially decoupled in the crystron. This obser-

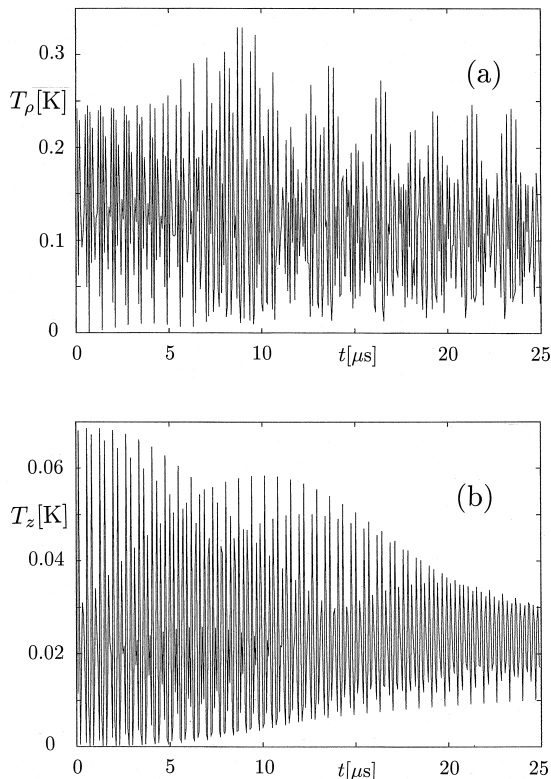


Fig. 3. Radial (a) and axial (b) temperatures of the 1000-ion chain as a function of time during the acceleration stage in the crystron.

vation, however, may only apply to quasi one-dimensional chains. More complicated three-dimensional ion structures [9–11] may couple these two degrees of freedom more effectively. We also note that the definition (7) of the crystal temperature contains the deterministic effects of the rf micromotion of the ring trap and the regular motion of the ions in the ring trap's pseudo-oscillator potential [37]. While we checked explicitly that the effect of the micromotion on the temperature is small, the violent temperature oscillations in Fig. 3 are most probably due to the ions' secular motion in the pseudo-oscillator. But since this oscillation does not qualitatively change the average behavior of the temperature of the crystal, we did not subtract this contribution from (7). It is essential to note that despite the additional contribution of the secular oscillations the temperature of the 1000-ion chain stays close to its initial temperature (well under 1K) during the entire acceleration phase. The most important result, however, is that the longitudinally ordered structure is preserved. This is already indicated by the fact that the radial and the axial temperatures do not increase (see Fig. 3). But in addition, a more convincing demonstration of the preservation of the ordered structure is provided in Fig. 2 (b). It shows the distribution of particle spacings of the 1000-ion chain at the end of the acceleration phase. Compared with the initial distribution (Fig. 2 (a)), Fig. 2 (b) shows that the final distribution of ion spacings is smoother, but its width remained narrow. This means that the ions stayed close to their equilibrium positions, approximately 30 μm apart.

Fig. 4 shows the rotational energy per particle as a function of time. This figure proves that the crystal is indeed accelerated and reaches a final energy of $E_f \approx 45.6$ eV which corresponds to a final velocity of $v_f \approx 19$ km/s. The final energy agrees well with a simple nonrelativistic estimate taking only the accelerating force $\mathbf{F}^{(A)}$ into account:

$$E_f = \frac{Z^2 e^2 R^2 B_0^2}{2m} = 45.6 \text{ eV}. \quad (8)$$

Eq. (8) shows that much larger final energies are obtained with larger accelerators. In our simulations we are currently limited to $N \approx 1000$ resulting in an accelerator of only $R \approx 0.5$ cm radius. According to

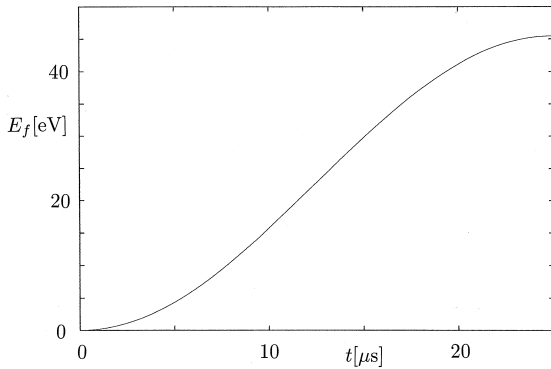


Fig. 4. Rotational energy per particle of the 1000-ion chain as a function of time during the acceleration stage in the crystron.

(8), however, an accelerator of the size of the MPQ ring trap or PALLAS (both approximately 5.75 cm radius) may already produce a final energy of $E_f \approx 6.6$ keV. The final energy is additionally increased by replacing the $^{24}\text{Mg}^+$ ions with lighter ions, e.g. $^7\text{Li}^+$ ions. Laser cooling of $^7\text{Li}^+$ ions has already been demonstrated [38]. The final energy for $^7\text{Li}^+$ ions in a mini crystron the size of the MPQ trap or PALLAS would already provide a final energy of $E_f \approx 23$ keV. Since (8) is directly proportional to Z^2/m , one may also think of using highly charged ions such as U^{92+} , or light charged particles such as electrons. In these cases laser cooling does not work and alternative cooling schemes have to be developed.

In addition to generating the initial crystalline ion configuration randomly as described above, we also ran simulations where we started with a hot ion plasma of up to $N = 1000$ ions and applied isotropic cooling by means of an additional damping force $\mathbf{F}^{(D)} = -\gamma \dot{\mathbf{r}}$ added to the right-hand side of (1). Choosing $\gamma = 10^{-3}$ we obtained self-consistently computed ion crystals that were taken as the initial conditions for the numerical simulation of the acceleration phase in the crystron. There was no qualitative change with respect to the results described earlier above. In particular, even in this more realistic simulation, we obtained stable, fast ion chains as a result of crystron acceleration.

Our simulations contain several approximations, simplifications and idealizations. (i) Quantum effect are not included in our simulations. This is justified

since even at 1 mK the ions are in such highly excited states that quantum effects are completely negligible. This, a posteriori, justifies our use of classical molecular dynamics simulations for the investigation of the stability of crystalline beams accelerated in the crystron. (ii) When stating the trap force (2), the toroidal shape of the ring trap was not taken into account. The ring trap was approximated as locally straight. We feel, however, that due to the small curvature of even a small crystron ($R \sim 1$ cm) this approximation is justified. (iii) Concerning the Coulomb force (3), we included all two-body interactions, although a large fraction of ions is blocked from interacting with a given ion by the ring-trap electrodes and the central structure of the crystron. But since the obscured ions are a macroscopic distance away from a given ion, it is unlikely that our ‘overcounting’ the interaction would qualitatively change our results. (iv) Our simulations do not yet take the effects of field imperfections, contact potentials and inaccuracies in the shape of the electrodes into account. A study of these effects is now under way and may prove crucial in view of the stability properties of actual experimental implementations of the crystron.

A final remark concerns the rise time of the magnetic field. In our simulations we assume $\omega = 0.002$ (see above) which was mainly dictated by computational considerations. Thus the magnetic field is ramped up from zero to its final value in a time interval $\Delta t = \tau_{\max} t_0 = 1/(2\omega f) = 25 \mu\text{s}$. This ramp time may seem short in comparison with rise times on the order of 20 ms frequently used in conventional betatrons [26]. However, with particle numbers ranging from $N = 50$ to $N = 200$ and ramp speeds ω ranging from 0.1 to 10^{-4} , we checked explicitly that a ramp time of 25 μs is already in the ‘adiabatic regime’, i.e., a longer ramp time will not result in a change of the final energy E_f of the crystals, nor will this longer acceleration time affect the stability properties of the acceleration stage.

Summarizing our results we produced beams of crystallized ions by implementing a reversal of the preexisting schemes for the production of crystalline beams. Instead of first accelerating the ions and subsequently cooling them, we propose to first crystallize the ions and *then* accelerate them. In order to accomplish this task, we propose a new type of

accelerator: the crystron. Using computer modelling, we have demonstrated stable acceleration of ion crystals in the crystron while preserving the crystalline structure. Cold crystalline beams of up to 1000 $^{24}\text{Mg}^+$ ions proved to be stable in the crystron. In addition we investigated the acceleration of a ‘hot’, but ordered ion chain consisting of 1000 $^{24}\text{Mg}^+$ ions. Even in this case we found stability and a final energy of the beam of $E_f \approx 45.6\text{ eV}$. Thus we have provided firm evidence, based on microscopic modelling of the acceleration phase of the crystron, that experimental implementation of the crystron may provide fast beams of crystallized heavy ions.

Acknowledgements

R.B. acknowledges financial support by NSF grant No. 9900730. P.E.S. acknowledges the Wesleyan REU program for financial support.

References

- [1] A.M. Mayer, *Am. J. Sci.* 15 (1878) 276, 477; 16 (1878) 247.
- [2] A.M. Mayer, *Nature* 17 (1878) 487; 18 (1878) 258.
- [3] J.J. Thomson, *Die Korpuskulartheorie der Materie*, Vieweg, Braunschweig, 1908.
- [4] L. Föppl, *J. reine angew. Math.* 141 (1912) 251.
- [5] R.F. Wuerker, H. Shelton, R.V. Langmuir, *J. Appl. Phys.* 30 (1959) 342.
- [6] F. Diedrich, E. Peik, J.M. Chen, W. Quint, H. Walther, *Phys. Rev. Lett.* 59 (1987) 2931.
- [7] D.J. Wineland, J.C. Bergquist, W.M. Itano, J.J. Bollinger, C.H. Manney, *Phys. Rev. Lett.* 59 (1987) 2935.
- [8] J.P. Schiffer, P. Kienle, *Z. Phys. A* 321 (1985) 181.
- [9] I. Waki, S. Kassner, G. Birkl, H. Walther, *Phys. Rev. Lett.* 68 (1992) 2007.
- [10] G. Birkl, S. Kassner, H. Walther, *Nature* 357 (1992) 310.
- [11] G. Birkl, S. Kassner, H. Walther, *Europhys. News* 23 (1992) 143.
- [12] M. Steck, K. Beckert, H. Eickhoff, B. Franzke, F. Nolden, H. Reich, B. Schlitt, T. Winkler, *Phys. Rev. Lett.* 77 (1996) 3803.
- [13] M. Steck, K. Beckert, H. Eickhoff, B. Franzke, F. Nolden, H. Reich, P. Spaedtke, T. Winkler, *Hyperf. Int.* 99 (1996) 245.
- [14] M. Steck, *Nucl. Phys. A* 626 (1996) 473.
- [15] D. Habs, R. Grimm, *Annu. Rev. Nucl. Part. Sci.* 45 (1995) 391.
- [16] N.S. Dikansky, D.V. Pestrikov, *The Physics of Intense Beams and Storage Rings* (American Institute of Physics Press, New York, 1994).
- [17] R.W. Hasse, *Theoretical Verification of Coulomb Order of Ions in a Storage Ring*, GSI-Preprint 99–23, July 1999.
- [18] T. Schätz, U. Schramm, D. Habs, *Hyperfine Interactions* 115 (1998) 29.
- [19] L.I. Schiff, *Rev. Sci. Inst.* 17 (1946) 6.
- [20] H. Primack, R. Blümel, *Eur. Phys. J. A* 3 (1998) 299.
- [21] H. Primack, R. Blümel, *Phys. Rev. E* 60 (1999) 957.
- [22] T.W. Hänsch, A.L. Schawlow, *Opt Commun.* 13 (1975) 68.
- [23] S. Stenholm, *Rev. Mod. Phys.* 58 (1986) 699.
- [24] D.W. Kerst, *Phys. Rev.* 60 (1941) 47.
- [25] D.W. Kerst, *Nature* 157 (1946) 90.
- [26] R. Kollath, *Teilchenbeschleuniger* (Friedr. Vieweg & Sohn, Braunschweig, 1962).
- [27] P.J. Bryant, K. Johnsen, *The Principles of Circular Accelerators and Storage Rings* (Cambridge University Press, Cambridge, 1993).
- [28] P.K. Ghosh, *Ion Traps* (Clarendon Press, Oxford, 1995).
- [29] D.J. Larson, J.C. Bergquist, J.J. Bollinger, W.M. Itano, D.J. Wineland, *Phys. Rev. Lett.* 57 (1986) 70.
- [30] J.W. Emmert, M. Moore, R. Blümel, *Phys. Rev. A* 48 (1993) 1757.
- [31] M.G. Moore, R. Blümel, *Physica Scripta T* 59 (1995) 434.
- [32] D.J. Wineland, private communication.
- [33] W. Quint, private communication.
- [34] R. Blümel, C. Kappler, W. Quint, H. Walther, *Phys. Rev. A* 40 (1989) 808.
- [35] H. Primack, R. Blümel, *Phys. Rev. E* 58 (1998) 6578.
- [36] R.W. Hasse, J.P. Schiffer, *Ann. Phys.* 203 (1990) 419.
- [37] H.G. Dehmelt, *Adv. Atom. Mol. Phys.* 3 (1967) 53.
- [38] S. Schröder, R. Klein, N. Boos, M. Gerhard, R. Grieser, G. Huber, A. Karafillidis, M. Krieg, N. Schmidt, T. Kühl, R. Neumann, V. Balykin, M. Grieser, D. Habs, E. Jaeschke, D. Krämer, M. Kristensen, M. Music, W. Petrich, D. Schwalm, P. Sigray, M. Steck, B. Wanner, A. Wolf, *Phys. Rev. Lett.* 64 (1990) 2901.